P1.1 BAROCLINICITY INFLUENCES ON STORM DIVERGENCE IN THE SUBTROPICS

Larry J. Hopper, Jr.*, and Courtney Schumacher
Texas A&M University, College Station, Texas

1. INTRODUCTION

Many studies have investigated how the vertical structure of divergence and diabatic heating associated with deep convection influences the large-scale dynamical response in the tropics. However, outside of individual case studies, the effect precipitating systems have on the large-scale circulation through variations in mesoscale divergence and diabatic heating is not well understood in the subtropics or midlatitudes. Recent case studies suggest that midlatitude convection may actually have an active feedback on the large-scale circulation**.** Bryan and Fritsch (2000) found that horizontal variations in diabatic heating within frontal storm systems intensify frontogenesis. Chang et. al (2002) also described how diabatic heating from condensational processes strengthen midlatitude storm tracks. Diabatic heating is nearly equal to the horizontal divergence in tropical convection (Mapes and Houze 1995). Thus, we can assume that variations in horizontal divergence in extratropical precipitating systems can also be related to the strength of fronts and storm tracks.

Divergence structures have been extensively studied within MCSs, particularly those consisting of a leading line of convection followed by a trailing stratiform rain area (hereafter referred to as LLTS-MCSs). These systems are found in both the tropics and midlatitudes. Gamache and Houze (1982) showed that the mean divergence profile for tropical LLTS-MCSs predominantly consists of low-level convergence and upper-level divergence with some weak surface divergence (see combined line in Fig. 1). The mean profile is a cross between the stratiform profile, which consists of moderate convergence centered at the 0°C level and moderate divergence at lower and upper levels, and the convective profile, which consists of strong low-level convergence and strong upper-level divergence. Stensrud and Anderson (2001) argued that persistent midlatitude convection caused by MCSs can produce source regions for Rossby waves that alter midlatitude circulation patterns. They further suggest that the continuous succession of MCSs during the 1993 Midwestern floods produced persistent upper-level divergence that encouraged low-level convection. Since LLTS-MCSs are an important source of rain in the subtropics, their horizontal divergence structures cannot be neglected when investigating the large-scale feedback precipitating systems have on the global circulation. However, this study also investigates the divergence structures of other common storm types in the subtropics for a more complete climatology of storm divergence.

*Corresponding author address: Larry J. Hopper, Jr., Department of Atmospheric Sciences, Texas A&M University, 3150 TAMU, College Station, TX 77843-3150; email: lhopper@ariel.met.tamu.edu.

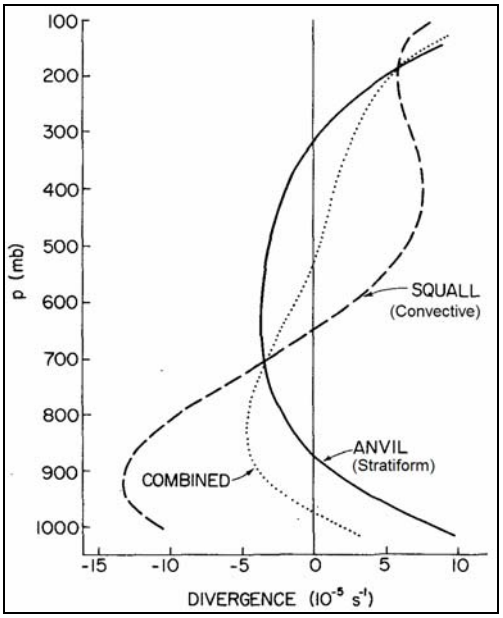

Figure 1: Mean divergence for the convective-squall line (dashed), stratiform-anvil (solid) and combined (dotted) regions of a tropical squall-line system (Adapted from Gamache and Houze 1982).

A mesoscale model is employed to compare the vertical variations in divergence patterns associated with convective and non-convective precipitating systems in southeast Texas. In addition, the precipitating systems are separated into categories based on the baroclinicity of the environment since southeast Texas is affected by both midlatitude (baroclinic) and tropical (barotropic) influences. This study uses the three environmental baroclinicity designations (barotropic, weakly baroclinic, and baroclinic) parameterized by Brugman and Schumacher (2005), which were based on NCEP Reanalysis daily mean surface temperatures over a 10 x 10 degree grid box centered over southeast Texas (25°N-35°N and 100°W-90°W). The baroclinicity classifications for each case in this study were checked for consistency with synoptic observations and by parameterizing baroclinicity designations on the same grid box using zonal wind fields. For each of the three baroclinicity designations, one well-modeled LLTS-MCS case and one well-modeled case resulting from another storm type are studied to determine the relative importance different baroclinic environments have on model-derived divergence profiles associated with varying storm types in the subtropics.

2. MODEL

Model simulations of each case were conducted using version 3 of the fifth-generation National Center

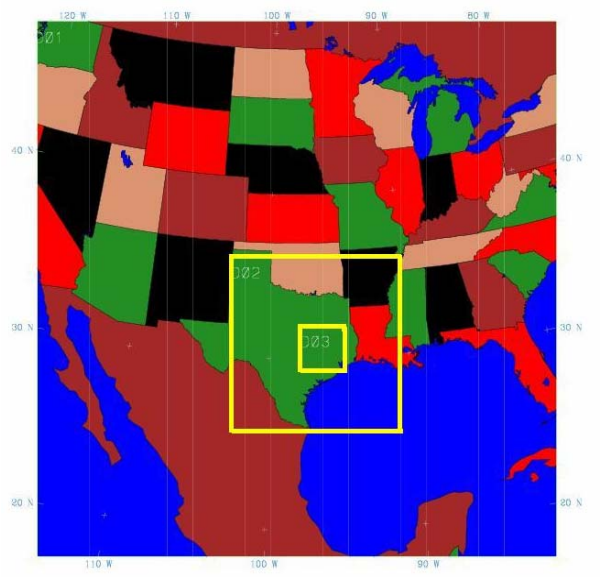

Figure 2: The relative locations of MM5 model domains. The grid increments of the outermost domain 1 (D1), domain (D2), and the innermost domain 3 (D3) are 27, 9, and 3 km, respectively.

for Atmospheric Research-Pennsylvania State University (NCAR-PSU) nonhydrostatic Mesoscale Model (MM5; Dudhia 1993). The 27-km outermost domain (D1) consists of 133 x 133 grid points with 23 vertical sigma levels covering the majority of the continental United States and Mexico (Fig. 2). The second domain (D2) consists of 130 x 130 grid points with 9-km grid spacing, while the inner-most 3-km domain (D3) consists of 100 x 100 grid points. The NCEP Global Final (FNL) Tropospheric Analysis is used to create the initial and lateral boundary conditions, and two-way nesting is utilized for the lateral boundary conditions of D2 and D3. The planetary boundary layer (PBL) was modeled using a high-resolution Blackadar scheme (Zhang and Anthes 1982), and radiative processes were handled using a scheme that accounts for longwave and shortwave interactions with other clouds and the clear atmosphere (Dudhia 1989).

The cumulus and microphysics schemes that generated the most realistic representation for each storm were utilized. The Grell cumulus parameterization scheme (Grell 1993) was used in all of the model runs except the weakly baroclinic LLTS-MCS, in which the Kain-Fritsch 2 cumulus parameterization scheme was used (Kain and Fritsch 1990; Kain 2003; Table 1). The only case that did not use a cumulus scheme on D2 was the strongly baroclinic case. A cumulus parameterization was not used on the inner-most domain (D3) for any case since the model is able to resolve convection explicitly with a 3-km grid spacing. Only the Reisner (Reisner et. al 1998) and Goddard (Tao and Simpson 1993) microphysics schemes, both of which include equations for predicting graupel, were utilized in this study. The organization of the convection, strength of the reflectivity in the vertical and horizontal, and distribution of rainfall were the primary factors that determined which model run was best. Some emphasis was also placed on the timing of convection and smaller scale features within the storm complexes. Future work will determine which model run is most appropriate in cases where multiple runs appear to perform equally well, although initial comparisons of these cases suggest different microphysics schemes only alter the mean structure of divergence and reflectivity minimally. Sensitivity tests will most likely be performed by comparing the vertical structure of reflectivity and divergence from ground-based radar data calculated using different microphysics and cumulus schemes from good model runs.

3. REFLECTIVITY AND DIVERGENCE

Reflectivity and horizontal divergence were calculated on D3 during the times for which rainfall was occurring within the inner-most domain. The outermost five grid boxes were not used in calculating the model-derived values for reflectivity and divergence due to inconsistencies between the resolved (D3) and parameterized (D2) rainfall along D3's outer boundary. Even though the strongly baroclinic case does not employ a cumulus parameterization on D2, the outermost five grid boxes were still discarded to maintain consistency with the other cases. Reflectivity calculations were based on the algorithm of Stoelinga (2005) except that fixed intercept parameters for rain, snow, and graupel were utilized as opposed to variable ones. Figures 3 and 5 compare the reflectivities taken from NEXRAD and the model-derived reflectivities for each case used in this study. The times represented by both the NEXRAD and model-derived radar images are not necessarily the same since the model occasionally developed convection at the wrong time. Rather, they represent similar times in the storm's evolution. Figures 4 and 6 show the vertical distribution of reflectivity for each storm; each line represents a 10% quantile (from 10-90%) of echo occurrence with height. The plots are cut off at levels that do not have an adequate number of reflectivity values (< 0.5% of the total count). The mean horizontal divergence for each grid box was calculated using the model-derived horizontal winds. The mean

Table 1: Cumulus and microphysics schemes and the model run duration for each case.

Storm Type	Model Run Period	D1 and D2 Cumulus Scheme	Microphysics Scheme
Barotropic LLTS-MCS	6/18/06 00Z-6/18/06 18Z	Grell	Reisner
Weakly Baroclinic LLTS-MCS	5/6/06 00Z-5/6/06 18Z	Kain-Fritsch 2	Goddard
Strongly Baroclinic LLTS-MCS	10/31/05 12Z-11/1/05 06Z	Grell	Goddard
Barotropic	7/4/06 00Z-7/5/06 00Z	Grell	Reisner
Weakly Baroclinic	5/14/06 00Z-5/15/06 00Z	Grell	Reisner
Strongly Baroclinic	2/25/06 00Z-2/26/06 00Z	Grell (none on D2)	Reisner

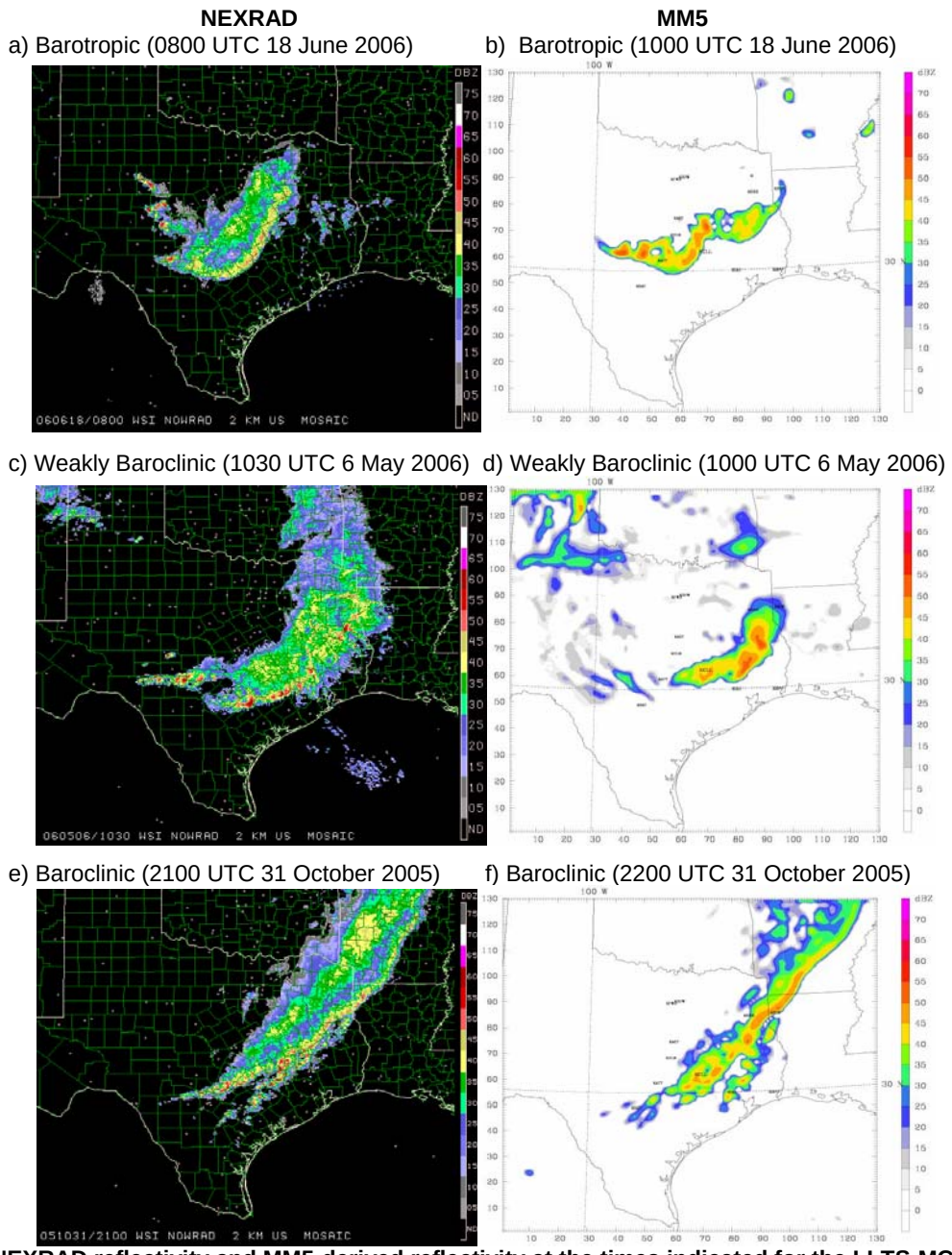

Figure 3: NEXRAD reflectivity and MM5-derived reflectivity at the times indicated for the LLTS-MCSs.

divergence profiles shown in Figs. 4 and 6 were calculated using divergence data in grid boxes where model-derived reflectivities were > 0 dBZ. Finally, mean heights for each sigma level were computed by inserting the mean model-derived surface temperature within D3 into the hydrostatic equation.

4. LEADING LINE-TRAILING STRATIFORM MCSs

4.1 *Barotropic LLTS-MCS*

The barotropic LLTS-MCS consisted of a bowed line with some smaller thunderstorms due to outflow behind the storm and the gust front ahead of the storm (Figs. 3a-b). It began as a cluster of storms that formed south of a weak surface front along the southwest Oklahoma-Texas border around 2200 UTC 17 June 2006 and propagated southeast due to northwest flow aloft into more unstable air. While a midlevel trough extended into central Texas, the LLTS-MCS moved into a more barotropic environment with small temperature gradients in southeast Texas, and was removed from most of the synoptic forcing present to the northwest.

The reflectivity distribution (Fig. 4a) shows tightly packed contours aloft (indicating more homogeneous

microphysical growth processes) with echo tops extending past 13 km and reflectivity values increasing toward the surface for most of the data, except in the bright band region ranging from 3.5 to 4.5 km. The mean divergence profile (Fig. 4b) is similar to the combined profile in Fig. 1 for a tropical squall line, but has a slightly higher level of non-divergence (LND) near 7km and magnitudes of convergence and divergence that are two to three times larger. The higher LND may occur since there may be more stratiform rain in this subtropical LLTS-MCSs than is found in tropical squall lines. The maximum low-level convergence is found slightly below the bright band near 3km, suggesting strong convection is probably present at and below this level. The profile becomes increasingly divergent with height and weak surface divergence is present due to outflow present along the gust front and behind the storm. The larger magnitudes of convergence and divergence may be reasonable since there is probably more synoptic forcing present in a barotropic subtropical LLTS-MCS than in a tropical LLTS-MCS.

4.2 *Weakly Baroclinic LLTS-MCS*

The weakly baroclinic LLTS-MCS was also a nocturnal bowed line (Figs. 3c-d) that differed from the barotropic LLTS-MCS in that it was more severe and formed from strong supercell thunderstorms. This storm also had a much larger region of stratiform rain than the barotropic LLTS-MCS, although the model does not make it as large as in reality. Numerous supercells formed in west Texas downstream of a midlevel shortwave along a stationary front around 2300 UTC 5 May 2006 and moved east. Supercells that were further northwest began organizing into a large MCS shortly thereafter, while supercells to the southeast remained severe until eventually merging with the LLTS-MCS around 0600 UTC 6 May. The stationary front draped west-to-east across central Texas had a larger temperature gradient than the barotropic case discussed in section 4.1.

The bright band feature shown in the reflectivity distribution (Fig. 4c) between 3 and 4 km is slightly lower than that found in the barotropic LLTS-MCS, indicative of the lower 0^{o}C level that would be expected earlier in the spring. Of the six cases utilized in this study, this case has the strongest reflectivities aloft with over 40 percent of the reflectivity values exceeding 35 dBZ at 8 km, suggesting a large amount of graupel formation, electrification, and strong updrafts characteristic of severe supercells and MCSs. The weakly baroclinic LLTS-MCS's divergence structure (Fig. 4d) is very similar to the barotropic LLTS-MCS divergence structure in Fig. 4b with strong low-level convergence and upper-level divergence, weak surface divergence, and a LND near 7km. The peak in convergence just below 3 km is slightly lower since the bright band feature is also lower. The magnitude of the upper-level divergence is twice as large as that found in the barotropic LLTS-MCS at 12 km and the magnitude of the lower-level convergence is also slightly larger. These results seem reasonable when compared to the barotropic LLTS-MCS since the convection is much stronger and the stratiform rain region is much larger in this case. The nice agreement between the structures of the barotropic and weakly baroclinic LLTS-MCSs and the idealized divergence structure for tropical squall lines (Fig. 1) suggests that the divergence calculations are reasonable and therefore can be applied to a wider variety of storm types not found in the tropics.

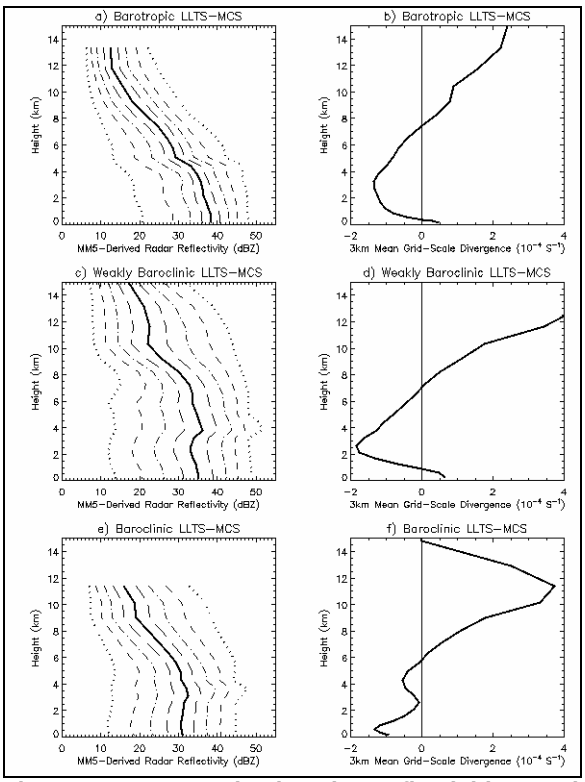

Figure 4: MM5-Derived radar reflectivities and horizontal divergence for the LLTS-MCSs used in this study.

4.3 *Strongly Baroclinic LLTS-MCS*

The baroclinic LLTS-MCS was an intense, frontal line of convection that had a fairly robust stratiform rain region throughout its duration (Figs. 3e-f). Unlike its barotropic and weakly baroclinic LLTS-MCS counterparts, this storm occurred during daytime hours and was accompanied by a very strong temperature gradient and strong midlevel trough characteristic of baroclinic systems. Convection began to form around 0500 UTC on 31 October 2005 near the southwest Kansas-Oklahoma border along a warm front and cold front extending from the surface low located there. The cold frontal convection evolved into a squall line and moved southeast during the day. By 2030 UTC as the squall line was passing through College Station, a large stratiform rain region had formed and some convection began to develop ahead

of the convective line. Both of these features were captured by the model output shown in Fig. 3f.

Like the weakly baroclinic LLTS-MCS, the reflectivity distribution for the baroclinic LLTS-MCS (Fig. 4e) displays a strong bright band between 3 and 4 km and some large reflectivity values aloft indicative of graupel formation and strong updrafts. However, measurable reflectivities only extend to around 11km and the surface reflectivities are generally weaker than the other LLTS-MCS cases. The convergence region for this baroclinic LLTS-MCS is not as elevated as those in the previous two cases, with the LND located between 5 and 6 km, likely because the convection is not as deep as it is in the other two LLTS-MCSs. Since the strength of the convection at upper levels as shown by the reflectivity distributions falls between that of the barotropic and weakly baroclinic LLTS-MCSs, the magnitude of the divergence aloft also falls somewhere between these other two cases. A major difference between this divergence profile and those of the barotropic and weakly baroclinic cases is that there is no near-surface divergence and convergence is maximized below 1km with a smaller convergence peak located near the bright band at 4 km. The low-level convergence suggests that convective processes dominate over stratiform processes in this system. The convergence minimum between 2 and 3 km suggests that the idealized convective profile shown in Fig. 1 is probably shifted downward in baroclinic, midlatitude MCSs. The lowered LND and differences in low-level convergence imply that the divergence structures in baroclinic LLTS-MCSs may be inherently different from those found in tropical squall lines and barotropic and weakly baroclinic subtropical LLTS-MCSs.

5. OTHER STORM TYPES

5.1 *Barotropic Case*

The barotropic case consisted of numerous air mass thunderstorms that rotated counterclockwise around a 500-700 mb closed low pressure system located in east-central Texas during the day on 4 July 2006 (Figs. 5a-b). Persistent convection over the previous three days may have contributed to the formation of this mesoscale low pressure system, whose origin is ambiguous since it is far removed from any large-scale features. Area soundings indicate an environment more characteristic of the tropics with weak shear, deep moisture and values of precipitable water above 60 mm. The model was able to capture the organizational mode of convection rotating around a low pressure system, but was not able to pinpoint the exact locations of cells due to their random, chaotic nature (Figs. 5a-b).

Unlike the barotropic LLTS-MCS discussed in section 4.1, the bright band in the reflectivity distribution for this case is weaker with over half the reflectivity data not even indicating a bright band (Fig. 6a). The reflectivity values below the 0^{o}C level increase towards the surface for the majority of the data since there is little or no evaporation in this extremely moist environment. Both of these features are characteristic of oceanic convection, in which stratiform rain results more from dying convective cells than large scale forcing. Therefore, the divergence profile for this barotropic case (Fig. 6b) agrees well with the idealized tropical convective profile shown in Fig. 1. The agreement between these profiles in low-level convergence peaks (~1.3×10^{-4} s^{-1}) and upper-level divergence maxima below 11 km (~7.0×10^{-5} s^{-1}) once again suggests that the model is producing reasonable wind values for divergence calculations. However, because the effects of stratiform rain are not negligible in tropical convection (Schumacher and Houze 2003), the LND is elevated to around 5 km and a weak maximum in convergence is found near 4 km where a weak bright band is located in the reflectivity distribution for this case.

5.2 *Weakly Baroclinic Case*

The weakly baroclinic case consisted of a west-to-east oriented line of discrete cellular convection with some stratiform rain resulting from decaying convection within the line (Figs. 5c-d). On 14 May 2006, strong convective cells began to form in far northeast Texas overnight (around 1000 UTC) along a stalled cold front to the southwest of a midlevel closed low pressure system centered over the Illinois-Indiana border. The cells progressed south through east Texas with the movement of the weak cold front, whose small temperature gradient was comparable to that in the weakly baroclinic LLTS-MCS case. The initial cells organized and split into two parts, with the western edge of the line containing stronger convection as indicated by the real and model-derived radar images (Figs. 5c-d).

The reflectivity distribution (Fig. 6c) suggests a mixture of microphysical growth processes due to the number of short-lived convective cells that left behind large areas of stratiform rain after decaying. Echo tops above 13 km and reflectivities exceeding 35 dBZ above the 0^{o}C level are representative of the strong convective cells present, while the bright band at 3 km and decreasing reflectivities toward the surface caused by weak evaporation are characteristic of the stratiform rain resulting from the decaying convection. The peak in convergence between 3 and 5 km (Fig. 6d) agrees with the location of the bright band. The large amount of divergence below 2 km and elevated LND near 8 km suggest this profile best matches the stratiform tropical divergence profile shown in Fig. 1. As in the weakly baroclinic LLTS-MCS case, the larger magnitudes of convergence and divergence found in this subtropical complex are most likely due to frontal forcing and the amount of deep convection present.

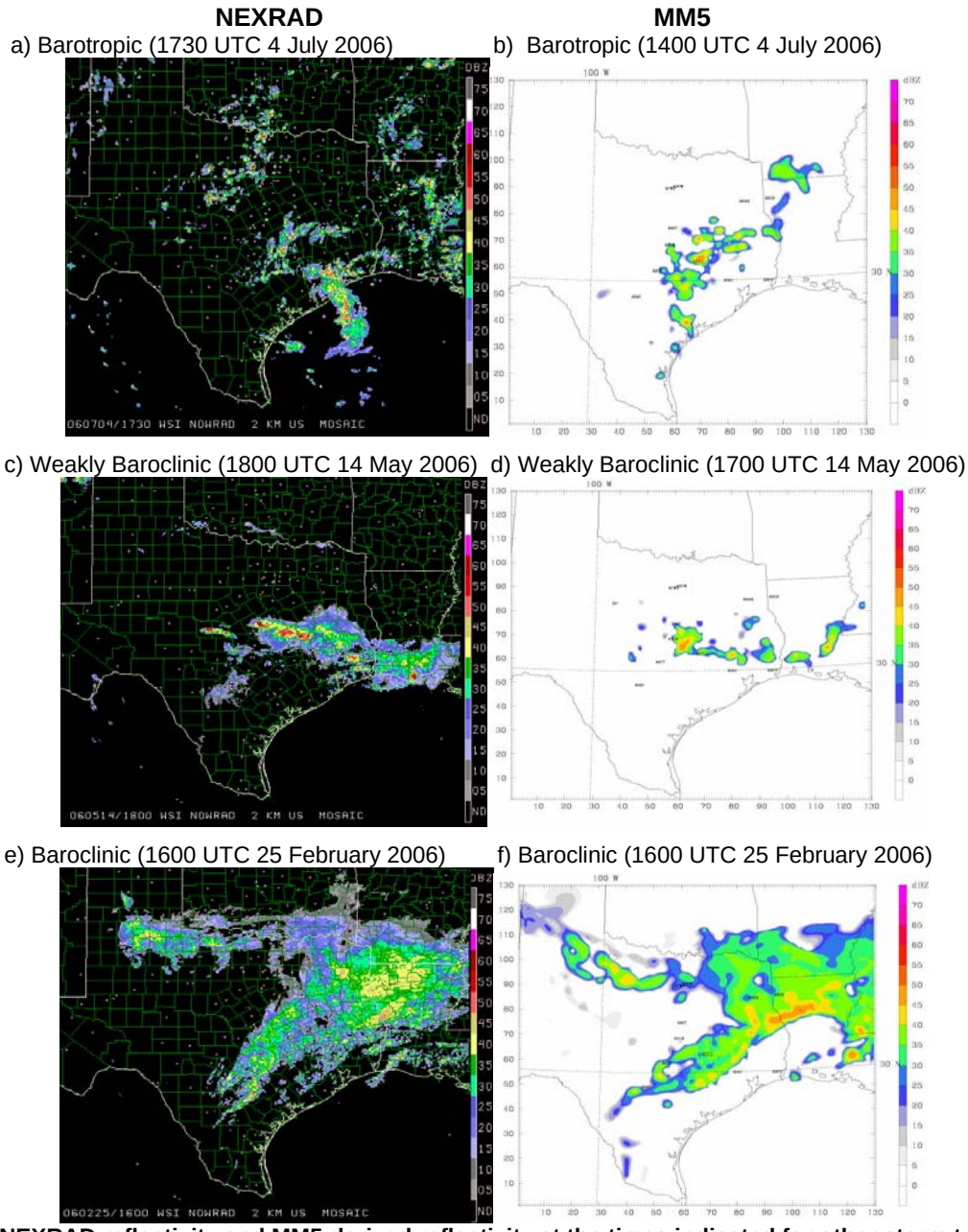

Figure 5: NEXRAD reflectivity and MM5-derived reflectivity at the times indicated for other storm types.

5.3 *Strongly Baroclinic Case*

The baroclinic case was a large stratiform rain region (characterized here as an MCS because of the extensive region of continuous rain) with a few areas of embedded convection (Figs. 5e-f) that formed downstream of a midlevel trough in an area of enhanced positive vorticity advection. A shortwave associated with this trough rapidly moved across Texas during 25 February 2006, further enhancing vorticity in the region. A cold front extending southwest from a low pressure system in Michigan was positioned in Oklahoma around 1200 UTC 25 February and moved quickly to the south, clearing the Texas gulf coast by 0100 UTC 26 February. The temperature gradient associated with the front, however, was not as large as would be expected for a baroclinic system since clearing directly north of the front allowed temperatures to be similar to areas in Texas ahead of the front experiencing rainfall from the MCS. However, there was a large temperature gradient in southern and southwest Texas where cloud cover from the MCS was not a factor in holding temperatures down for the majority of the day. Therefore, while other storms may better represent a baroclinic environment, the synoptic forcing from the midlevel trough makes the baroclinic designation for this storm reasonable.

This case had the weakest convection of all the cases in the study as indicated by the reflectivity distribution (Fig. 6e), which shows very little strong reflectivities above the 0^0C level and convection only extending to 10 km. The bright band between 2 and 3 km and the rapid decrease in reflectivities below it due to evaporation indicate that the rainfall in the MCS was largely stratiform. The divergence profile for this baroclinic case (Fig. 6f) is shifted downward from the other cases as indicated by the lower convergence maximum at 2 km and lower LND at 4 km. This result is reasonable since the tropopause level should be lower for this case than any of the other cases, thus compacting the entire divergence profile. Since little convection is present, this case has the smallest magnitude of low-level convergence (~7.0 x 10^{-5} s^{-1}) in the study. The magnitude of the divergence aloft (~2.0 x 10^{-4} s^{-1}) is comparable to the weakly baroclinic case and stronger than the barotropic case because of the stronger synoptic forcing.

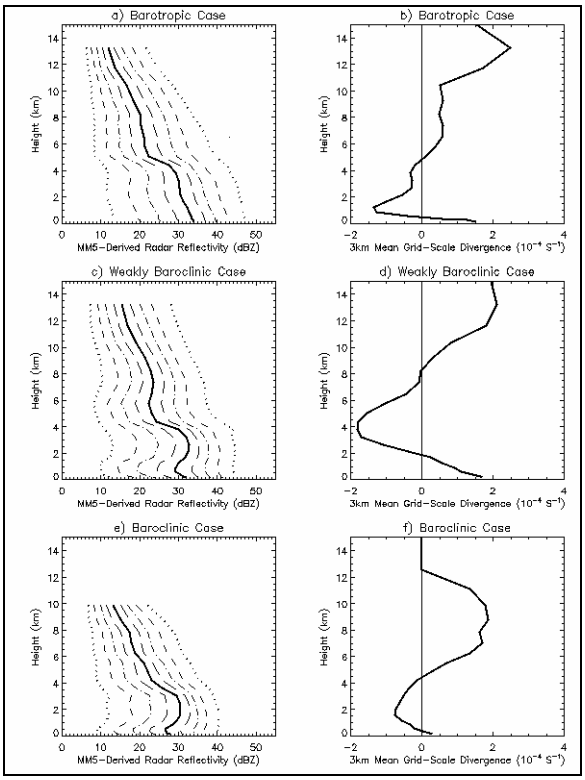

Figure 6: MM5-Derived radar reflectivities and horizontal divergence for the other storm types used in this study.

6. SUMMARY AND FUTURE WORK

Different divergence profiles are produced from varying degrees of baroclinicity and storm types in southeast Texas. The structures of mean divergence within the barotropic and weakly baroclinic LLTS-MCSs were very similar to the combined profile for tropical squall line systems found by Gamache and Houze (1982; Fig. 1). This suggests that the MM5-derived profiles are reasonable and therefore can be applied to a wider variety of storm types in the subtropics. The more convective nature of the baroclinic LLTS-MCS's divergence profile suggests that frontal LLTS-MCSs are dissimilar from squall lines caused by weaker synoptic forcing. It also may indicate that the effects of convective rain are more important than stratiform rain within frontal LLTS-MCSs.

Based on the six modeled cases, which included both well-organized MCSs and other types of precipitating systems, barotropic cases appeared to have higher LNDs (caused by high tropopause levels) and smaller magnitudes of upper-level divergence since synoptic forcing is weakest in these environments. The largest magnitudes of low-level convergence were found in the weakly baroclinic cases since they had large stratiform rain regions coupled with intense convection due to frontal forcing. Both baroclinic cases contained lower LNDs (caused by low tropopause levels) and smaller magnitudes of low-level convergence since convection is not as deep as it is in less baroclinic environments. While more cases need to be evaluated to conclude that the differences in storm divergence between varying baroclinic environments are real and meaningful from a climatological standpoint, these results point toward the importance of investigating this problem further.

In addition to including more cases, future work will focus on studying divergence within objectively determined stratiform and convective rain regions and how they vary by baroclinicity. Verification of the model-derived reflectivity and divergence fields also needs to be performed using ground-based radar data. Finally, since the degree of baroclinicity appears to cause different divergence structures, the dynamic response caused by these divergence profiles needs to be evaluated first over short time scales (by experimenting with nest interactions in MM5) and then perhaps extended to longer time and space scales by using longer integrations of regional or global models.

7. ACKNOWLEDGEMENTS

We thank Jason Sippel for having the patience to help us properly configure MM5 and for editing parts of this manuscript. Shuguang Wang and Neil Smith provided a tremendous amount of technical support. Finally, Zhiyong (Ellie) Meng contributed through numerous helpful discussions. This research is supported by NSF grant ATM-0449782.

8. REFERENCES

Brugman, K. E., and C. Schumacher, 2005; Variations in drop-size distributions associated with the degree of baroclinicity of the environment. *11th Conference on Mesoscale Processes*, October 24-29, Albuquerque, NM.

Bryan, G. H., and J. M. Fritsch, 2000: Diabatically driven discrete propagation of surface fronts: A numerical analysis. *J. Atmos. Sci.,* **57,** 2061-2079.

Chang, E. K., S. Lee, and K. L. Swanson, 2002: Storm track dynamics. *J. Climate*, **15,** 2163-2183.

Dudhia, J., 1989: Numerical study of convection observed during the Winter Monsoon Experiment using a mesoscale two-dimensional model. *J. Atmos. Sci.*, **46**, 3077-3107.

----------, 1993: A nonhydrostatic version of the Penn State-NCAR Mesoscale Model: Validation tests and simulation of an Atlantic cyclone and cold front. *Mon. Wea. Rev.*, **121,** 764-787.

Gamache, J. F., and R. A. Houze, Jr., 1982: Mesoscale air motions associated with a tropical squall line. *Mon. Wea. Rev.*, **110,** 118-135.

Grell, G.A., 1993: Prognostic evaluation of assumptions used by cumulus parameterizations. *Mon. Wea. Rev.*, **121,** 764-787.

Kain, J.S., 2003: The Kain-Fritsch convective parameterization: An update. *J. Appl. Meteor.*, **43,** 170-181.

----------, and J.M. Fritsch, 1990: A one-dimensional entraining/detraining plume model and its application in convective parameterization. *J. Atmos. Sci.*, **47,** 2784-2802.

Mapes, B. E., and R. A. Houze, Jr., 1995: Diabatic divergence profiles in western Pacific mesoscale convective systems. *J. Atmos. Sci.*, **52,** 1807-1828.

Reisner, J., R. M. Rasmussen, and R. T. Bruintjes, 1998: Explicit forecasting of supercooled liquid water in winter storms using the MM5 mesoscale model. *Quart J. Roy. Meteor. Soc.*, **124B,** 1071-1107.

Stensrud, D. J., and J. L. Anderson, 2001: Is midlatitude convection an active or passive player in producing global circulation patterns? *J. Climate*, **14,** 2222-2237.

Stoelinga, M., 2005: Simulated equivalent reflectivity factor as currently formulated in RIP: Description and possible improvements. White paper, 5 pgs.

Tao, W.-K., and J. Simpson, 1993: Goddard cumulus ensemble model. Part I: Model description. *Terr. Atmos. Oceanic Sci.*, **4,** 25-72.

Zhang, D. L., and R. A. Anthes, 1982: A high-resolution model of the planetary boundary layer---Sensitivity tests and comparisons with SESAME-79 data. *J. Appl. Meteor.*, **21,** 1594-1609.